Materials Research Proceedings 41 (2024) 688-695 https://doi.org/10.21741/9781644903131-76

Mechanical behavior and flow curve modeling of AZ31B magnesium alloy under low frequency vibration assisted tension

TIAN Ye[1,a], WEN Zhang[1,b], SHEN Weicai[1,c], ZHUANG Xincun[1,d*], ZHAO Zhen[1,e*]

[1]Institute of Forming Technology and Equipment, NERC of Die & Mold CAD,School of Materials Science and Engineering, Shanghai Jiao Tong University, Shanghai, 200030, China

[a]sjtutianye@sjtu.edu.cn, [b]w_zhang@sjtu.edu.cn, [c]weicaishen@sjtu.edu.cn
[d]georgezxc@sjtu.edu.cn, [e]zzhao@sjtu.edu.cn

Keywords: Low Frequency Vibration, Mechanical Behavior, Vibration Hardening, Flow Curve Model

Abstract. This study aimed to investigate the impact of the low-frequency vibration field on the mechanical behavior of AZ31B magnesium alloy. To achieve this, a series of low-frequency vibration-assisted tensile tests were conducted at room temperature. The effect of various vibration parameters on the mechanical characteristics of AZ31B was studied. The findings indicate that the introduction of low-frequency vibration field during the traditional tensile process leads to periodic oscillations in the flow stress of the material. Moreover, the maximum stress value was greater than the condition without vibration. The vibration hardening value is not significantly affected by the vibration frequency, but rather depends on the amplitude. The magnitude of the vibration hardening value increases with the increasing amplitude, and this relationship is non-linear. On this basis, a modified Hockett-Sherby hardening model was constructed by incorporating the vibration parameters. Statistical analysis of stress-strain curve, vibration hardening and stress fluctuation values were conducted to identify the model parameters. By comparing with the experimental result, the stress change of AZ31B magnesium alloy under low frequency vibration tension could be well predicted by this model.

Introduction

Vibration-assisted plastic forming technology is a new plastic forming method developed in vibration utilization engineering in recent years [1]. It utilizes the stress field and vibration energy field generated by vibration to reduce the load, increase the forming limit and improve the forming quality of the parts [2]. Cao et al. [3] studied 6061 aluminum alloy and found that after applying ultrasonic vibration, the evolution of dislocations was positively regulated, resulting in a decrease in deformation resistance. The level of stress reduction was proportional to the amplitude of ultrasonic waves. Ultrasonic vibration softening was mainly caused by stress superposition and acoustic softening effect. Han et al. [4] proposed a new tool-workpiece combined vibration ultrasonic micro-extrusion process, which can reduce the micro-extrusion stress, extend the extrusion length, enhance the grain deformation effect and generate fiber streamline. Deng [5] et al. applied low-frequency vibration field in T2 pure copper compression and found that low-frequency vibration increased the dislocation density in the material and promoted the formation of dislocation cells. The dislocation cells gradually evolved into new grain boundaries, and the grains were refined. Lin et al. [6] conducted 10 Hz and 0.3 mm amplitude low-frequency vibration assisted compression tests on Ti45Nb titanium alloy. The low-frequency vibration field promoted the dislocation motion and grain rotation, making the material's deformation more uniform and reducing the probability of crack nucleation.

In order to deeply understand the impact of vibration field on the mechanical behavior of materials and describe the mechanical response of materials under vibration conditions, it is necessary to establish a proper constitutive equation. At present, researchers have conducted

extensive research on the construction of models for vibration plastic forming. Meng et al. [7] established a hybrid constitutive model based on dislocation evolution theory, which can respectively describe the stress superposition and acoustic softening effects under the action of ultrasonic vibration field. Based on the theory of crystal plasticity, thermal activation and dislocation evolution, Yao et al. [8] proposed an acoustic model considering softening and residual effects, and calibrated it by ultrasonic vibration-assisted compression test. Through the study of 6063 aluminum alloy, Xie et al. [9] established a constitutive model for ultrasonic vibration compression based on the Johnson Cook model. Prabhakar et al. [10] extended the constitutive model based on dislocation density to the softening model induced by ultrasonic effect by superimposing transverse ultrasonic vibration in the tensile experiment of aluminum alloy. The predicted results are in good agreement with the experimental results. Zhang et al. [11] introduced the mechanical work done by low-frequency vibration, the critical vibration energy value and Hooke's law into the framework of thermal activation to establish the physical intrinsic structure from the perspective of thermal activation.

To investigate the effect of low-frequency vibration field on mechanical behavior of AZ31B magnesium alloy, this study conducted a series of room temperature low-frequency vibration assisted tensile tests. The investigation focused on analyzing the impact of various vibration parameters on the mechanical behavior of AZ31B. Subsequently, a flow curve model incorporating the vibration parameters was developed. A modified Hockett-Sherby hardening model was constructed by statistical analysis of stress-strain curve, vibration hardening value, stress fluctuation value, etc.

Material and experimental setup

The material used in this study is commercial AZ31B-H24 magnesium alloy sheet, and its chemical composition is shown in Table 1. The thickness of the as-received sheet is 2 mm. The tensile specimens were designed according to ASTM standards and prepared along the rolling direction of the as-received sheet. The specific dimensions are shown in Fig. 1a.

The experimental platform mainly consists of an electronic material testing machine (UTM5105) and an electro-hydraulic servo excitation device, which can accurately control low-frequency vibration within the frequency range of 0-50 Hz and amplitude range of 0-1 mm. The specific device is shown in Fig. 1b. The hydraulic control unit can provide a maximum excitation force of up to 200 kN. In order to ensure the reliability of data during the vibration process, the collection frequency of the electronic testing machine was set to 330 Hz. The strain of the material was measured using the digital image correlation (DIC) method. All test images were recorded with a pair of cameras from GOM's ARAMIS optical strain measurement system. The resolution of the cameras was 2752 × 2200 pixels and the system was calibrated to have a reference area of 100 × 100 mm. Considering that the superposition of low-frequency vibration will only make the material produce small elastic deformation, but will not change the deformation mode and stress state of the material. The acquisition frequency of three frames per second was used in this study, which can accurately record the strain condition during the tensile process to meet the requirements of strain testing.

The tensile speed in the quasi-static tensile test was 2 mm/min, with a strain rate of approximately 5×10^{-4}/s. In order to improve the accuracy of the experiment, the entrance force of the testing machine was set to 50 N, and after each experiment, the crossbeam of the testing machine automatically resets to the position before the last test started. The vibration device was activated when the material was stretched to 5% strain for 60 s, and finally stopped at 10% strain. The amplitude range used in this experiment was 0-0.1 mm and the frequency range was 0-30 Hz. The specific testing conditions are shown in Table 2, and each experiment should be tested at least three times to ensure the reproducibility of the experiment.

Table 1. Chemical composition of As-received AZ31B-H24 (in wt%).

Al	Zn	Mn	Si	Fe	Cu	Ni
3.10	0.91	0.31	0.02	0.00	0.00	0.00

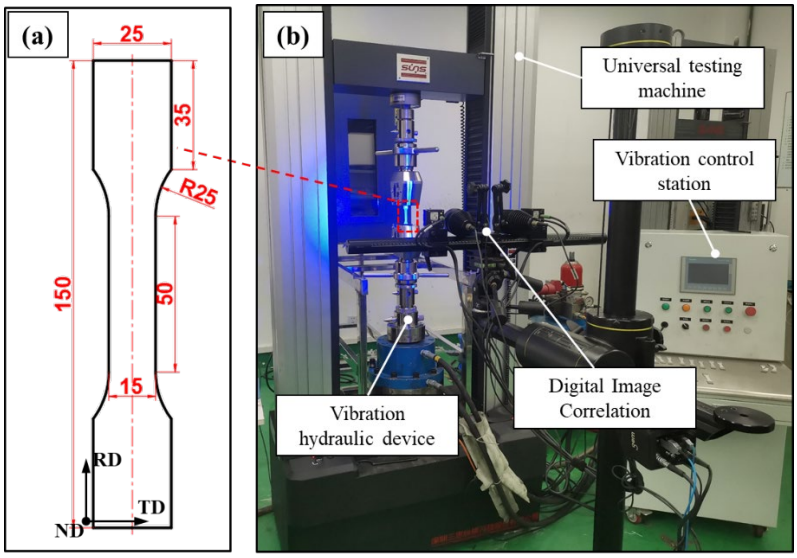

Fig.1 Schematics of the tension specimen (a) and experimental setup (b).

Table 2. Conditions of the LFVT tests.

Item	Condition
Material	AZ31B-H24
Effect of amplitude	0/0.025/0.05/0.075/0.1 mm, 20 Hz
Effect of frequency	0.075 mm, 0/10/20/30 Hz

Mechanical behavior under LFVT

Fig. 2a shows a comparison of the curves with and without vibration, and it can be found that the two curves basically overlap before the superimposed low-frequency vibration. Once low-frequency vibration was applied, the stress exhibits periodic fluctuations, which is called the stress superposition effect [12]. The stress superposition effect was first proposed by Nevill and Brotzen [13], who suggested that the average load drop in ultrasonic vibration is attributed to the superposition mechanism of steady and alternating stresses. Relevant researchers believe [14,15] that the effect is also applicable to low-frequency vibration, and the metal under the low-frequency field will also produce a nonlinear response of stress caused by loading and unloading, which is directly related to the elasticity of the material. Deng et al. [5] elucidated the stress superposition effect from the perspective of the stress wave, and the fluctuating stress field will be generated inside the metal material under the low-frequency vibration field, and the effect will certainly exist in the in vibroforming. In the uniaxial tensile process, the low-frequency vibration field produces periodic stress fluctuations in the stress component along the tensile direction, but does not cause changes in the plastic deformation mechanism or internal microstructure of the material.

From the above, it can be seen that during a single oscillation period, there is an upper limit denoted as σ_{max} and a lower limit denoted as σ_{min} for the flow stress. The disparity between these two values is defined as the stress fluctuation, which can be mathematically expressed as $\Delta\sigma =$

$\sigma_{max} - \sigma_{min}$. The effects of amplitude and frequency on $\Delta\sigma$ are depicted in Fig. 2b and c, respectively. It is clear from the data that $\Delta\sigma$ is positively correlated with the increase in amplitude. However, changing the vibration frequency does not have a substantial effect on $\Delta\sigma$.

Furthermore, it has been observed from Fig. 2a that the peak of the oscillation curve exceeded the traditional tensile flow stress, indicating the presence of the vibration hardening phenomenon in the LFVT process. To quantitatively assess the impact of vibration hardening, a metric termed the vibration hardening value *S* was introduced, which is represented as the discrepancy between the maximum value (σ_{max}) of the oscillation curve and the flow stress (σ_{WV}) corresponding to that particular point in without vibration tension, that is, $S = \sigma_{max} - \sigma_{WV}$. The statistical results of *S* are presented in Table 3. It is noteworthy that the vibration frequency does not exert a direct impact on the vibration hardening value *S*. Similar to $\Delta\sigma$, the vibration hardening value *S* is primarily influenced by the magnitude of the amplitude. This means that as the amplitude increases, the vibration hardening value *S* also increases. The amplitude plays a crucial role in determining the magnitude of *S*.

To sum up, whether it is for $\Delta\sigma$ or *S*, the impact of vibration frequency is much smaller than the amplitude. Similar conclusions have been drawn by other researchers regarding the influence of vibration frequency on mechanical behavior [5, 16].

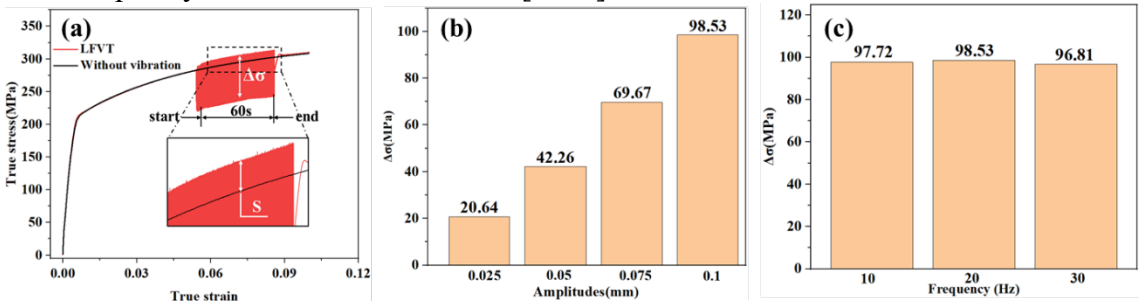

Fig. 2 True stress–strain curves under LFVT(a), effect of amplitude on stress fluctuation values(b), effect of frequency on stress fluctuation values(c).

Table 3. Average vibration hardening value S

	Effect of amplitude				Effect of frequency		
Amplitude(mm)	0.025	0.05	0.075	0.1	0.075		
Frequency (Hz)	20				10	20	30
***S*(MPa)**	5.67	9.09	11.38	13.40	11.21	11.38	11.16

Flow curve modeling of mechanical behavior under LFVT

The Hockett-Sherby hardening model is a type of saturation model, meaning that as the strain increases, the flow stress reaches a constant value. The original expression for the Hockett-Sherby hardening model is as follows:

$$\sigma = \sigma_s - (\sigma_s - \sigma_i) \times \exp(-a\varepsilon^n) \quad (1)$$

In equation (1), σ_s is the saturation stress; σ_i is the initial yield stress; *a* and *n* are constants ($a > 0$). The parameters of the model (σ_s, σ_i, *a* and *n*) can be determined by applying the results of static tensile tests to the Hockett-Sherby hardening model.

$$\sigma = 336.14 - 123.7 \times \exp(-12.09 \times \varepsilon^{0.87}) \quad (2)$$

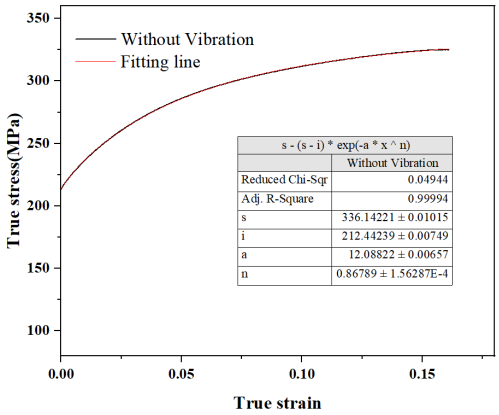

Fig.3 Fitting results of flow stress using the Hockett-Sherby model

When low-frequency vibration was applied, the flow stress of the material undergoes oscillations between the maximum and minimum values. This stress fluctuation, denoted as $\Delta\sigma$, was primarily caused by the elastic loading and unloading of the vibration. According to Hooke's law, it can be inferred that the expression for $\Delta\sigma$ is as follows:

$$\Delta\sigma = \sigma_{max} - \sigma_{min} = c \times \frac{EA}{L} \tag{3}$$

Here, $\frac{EA}{L}$ represents the variation in strain induced by the applied vibration; c is constant; E is elastic modulus (for magnesium alloys, the value is 45 GPa); L is specimen gauge length (50 mm). Based on the results shown in Fig. 2b, a $\Delta\sigma$ - EA/L relationship can be constructed as shown in Fig. 4. The slope of the fitted curve represents the coefficient c. Therefore, the specific expression for the $\Delta\sigma$ is given by:

$$\Delta\sigma = 981 \times A \tag{4}$$

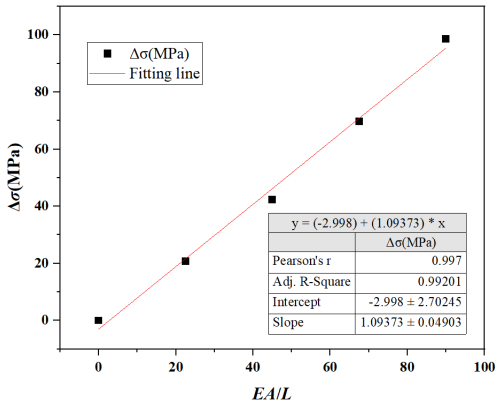

Fig. 4 Linear fitting results of Δσ - EA/L during LFVT

To further understand the relationship between the vibration hardening value S and the amplitude A, a vibration hardening coefficient function $f(A)$ was constructed. The equation (5) represents the relationship between S and $f(A)$, and is given as follows:

$$S = \sigma_{max} - \sigma_{wv} = \sigma_{wv} \times f(A) - \sigma_{wv} \tag{5}$$

Due to the magnitude of S is determined by the amplitude A. By varying the amplitude, we can observe the corresponding changes in the vibration hardening value. Therefore, it can be deduced that $f(A)$ also depends on the amplitude A. The specific expression for $f(A)$ is as follows:

$$f(A) = \left\{k \times (\frac{A}{A_0})^q + 1\right\}^m \tag{6}$$

where A denotes the amplitude; A_0 refers to reference amplitude (whose value is 1mm); k is constants; m and q are constants. Obviously, when $A = 0, f(0) = 1$. The σ_{max}/σ_{wv} - A/A_0 relationship was established and shown in Fig. 5. According to the fitting results, a mathematical expression about $f(A)$ was obtained:

$$f(A) = (2.27 \times A^{0.66} + 1)^{0.11} \tag{7}$$

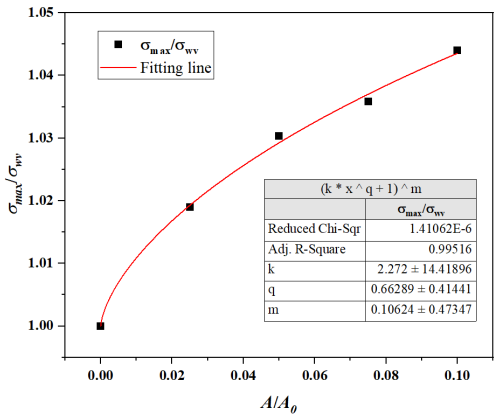

Fig. 5 Linear fitting results of σ_{max}/σ_{wv}-A/A_0

The fitting results of the modified Hockett-Sherby hardening model parameters are summarized in Table 4.

Table 4. Parameters of modified Hockett-Sherby model

parameters	σ_s(MPa)	σ_i(MPa)	a	n	k	q
value	336.14	212.44	12.09	0.87	2.27	0.66
parameters	m	c	E(GPa)	L(mm)	A_0(mm)	
value	0.107	1.09	45	50	1	

In summary, when low-frequency axial vibration was applied to AZ31B magnesium alloy, the curve of stress variation with strain of the material can be described by equation (8) :

$$\begin{cases} \sigma_{max} = \{\{336.14 - 123.7 \times \exp(-12.09 \times \varepsilon^{0.87})\} \times (2.27 \times A^{0.66} + 1)^{0.11} \\ \sigma_{min} = 336.14 - 123.7 \times \exp(-12.09 \times \varepsilon^{0.87}) \times (2.27 \times A^{0.66} + 1)^{0.11} - \Delta\sigma \\ \Delta\sigma = 981 \times A \end{cases} \tag{8}$$

To verify the accuracy of the model, the LFVT results with an amplitude of 0.06 mm and a frequency of 20 Hz were compared with the predicted results. The comparison result is shown in Fig. 6. The results demonstrated that the model accurately captures the mechanical behavior of AZ31B under LFVT. This suggests that the Hockett-Shelby hardening model coupled with vibration parameters can provide valuable insights into the mechanical behavior of materials during vibration-assisted deformation.

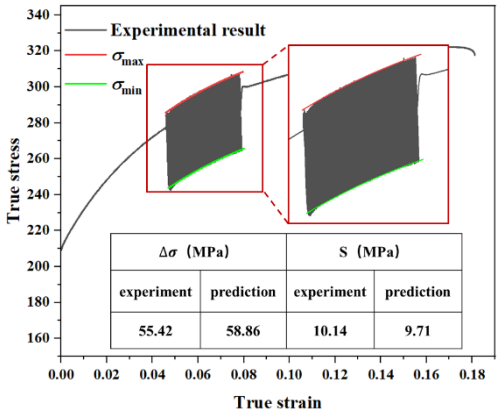

Δσ (MPa)		S (MPa)	
experiment	prediction	experiment	prediction
55.42	58.86	10.14	9.71

Fig. 6 Comparison between predicted results of models and experimental results.

Conclusion

This study conducted LFVT tests on AZ31B sheet and investigated the effects of amplitude and frequency on mechanical behavior. On this basis, a Hockett-Sherby model coupled with vibration parameters was established and validated. The main conclusions are as follows:

(1) With superimposed low-frequency vibration field, the flow stress curve has the characteristic of stress oscillation phenomenon caused by periodic loading and unloading. The value of stress fluctuation increases with the increasing amplitude. For AZ31B magnesium alloy, low-frequency vibration field causes vibration hardening, and the variation trend is basically consistent with the fluctuation stress value. Compared with amplitude, vibration frequency has less effect on the mechanical behavior.

(2) Within the framework of Hockett-Sherby hardening model, the impact of amplitude was involved, and the parameters were determined through statistical analysis of the aligning quasi-static tensile stress-strain curve, stress fluctuation value, and vibration hardening value. By taking the amplitude effect into account, the Hockett-Sherby hardening model effectively forecasts the mechanical behavior of AZ31B under LFVT.

References

[1] T. Maeno, K. Osakada. K. Mori, Reduction of friction in compression of plates by load pulsation[J]. Int. J. Mach. Tool. Manu., 51 (2011) 612-617. https://doi.org/10.1016/j.ijmachtools.2011.03.007

[2] Z. Yao, G. Kim, L. Faidley, L. Faidley, Q. Zou, D. Mei, Z. Chen, Effects of superimposed high-frequency vibration on deformation of aluminum in micro/meso-scale upsetting[J]. J. Mater. Process. Tech., 212 (2012) 640-646. https://doi.org/10.1016/j.jmatprotec.2011.10.017

[3] M. Cao, H. Hu, X. Jia, S. Tian, C. Zhao, X. Han, Mechanism of ultrasonic vibration assisted upsetting of 6061 aluminum alloy[J]. J. Manuf. Process., 59 (2020) 690-697. https://doi.org/10.1016/j.jmapro.2020.09.070

[4] G. Han, W. Wan, Z. Zhang, L. Xu, F. Liu, H. Zhang, Experimental investigation into effects of different ultrasonic vibration modes in micro-extrusion process[J]. J. Manuf. Process., 67 (2021) 427-437. https://doi.org/10.1016/j.jmapro.2021.05.007

[5] L. Deng, P. Li, X. Wang, M. Zhang, J. Li, Influence of low-frequency vibrations on the compression behavior and microstructure of T2 copper[J]. Mater. Sci. Eng. A, 710 (2018) 129-135. https://doi.org/10.1016/j.msea.2017.10.083

[6] J. Lin, C. Pruncu, L. Zhu, J. Li, Y. Zhai, L. Chen, Y. Guan, G. Zhao, Deformation behavior and microstructure in the low-frequency vibration upsetting of titanium alloy[J]. J. Mater. Process. Tech., 299 (2022) 117360. https://doi.org/10.1016/j.jmatprotec.2021.117360

[7] B. Meng, B. Cao, M. Wan, C. Wang, D. Shan, Constitutive behavior and microstructural evolution in ultrasonic vibration assisted deformation of ultrathin superalloy sheet[J]. Int. J. Mech. Sci., 157 (2019) 609-618. https://doi.org/10.1016/j.ijmecsci.2019.05.009

[8] Z. Yao, G. Kim , Z. Wang , L. Faidley, Q. Zou, D. Mei, Z. Chen, Acoustic softening and residual hardening in aluminum: modeling and experiments[J]. Int J Plast., 39 (2012) 75-87. https://doi.org/10.1016/j.ijplas.2012.06.003

[9] Z. Xie, Y. Guan, J. Lin, J. Zhai, L. Zhu, Constitutive model of 6063 aluminum alloy under the ultrasonic vibration upsetting based on Johnson-Cook model[J]. Ultrasonics, 96 (2019) 1-9. https://doi.org/10.1016/j.ultras.2019.03.017

[10] A. Prabhakar, G.Verma, K. Hariharan, P. Pandey, M. Lee, S. Suwas, Dislocation density based constitutive model for ultrasonic assisted deformation[J]. Mech. Res. Commun. 85 (2017) 76-80. https://doi.org/10.1016/j.mechrescom.2017.08.003

[11] W. Zhang , Y. Xu, Q. Li, X. Zhuang, Z. Zhao, Constitutive modeling and deformation analysis of W-temper and peak aged 7075 alloy sheets under low frequency vibration assisted tension[J]. Int. J. Mech. Mater. Des., 19 (2023) 583-604. https://doi.org/10.1007/s10999-023-09647-8

[12] Y. Xu, X. Zhuang, W. Zhang, Q. Li, Z. Zhao, Mechanical behaviors and microstructure characteristics of W-tempered and peak-aged 7075 alloy sheets under low frequency vibration–assisted tension[J]. Mater. Sci. Eng. A, 833 (2022) 142338. https://doi.org/10.1016/j.msea.2021.142338

[13] G. Nevill, F. Brotzen, The effect of vibrations on the static yield strength of a low-carbon steel[J]. Proceedings of American Society for Testing Material, 57 (1957) 751-758.

[14] P. Li, X. Wang, M. Zhang, L. Deng, J. Jin, Compression deformation behavior and size effect of copper under low-frequency vibration [J]. Forging & Stamping Technology. 42 (2017) 140-145

[15] D. Meng, J. Ma, X. Zhao, Y. Guo, C. Zhu, M.Yu, Mechanical behavior and material property of low-carbon steel undergoing low-frequency vibration-assisted upsetting[J]. J. Mater. Res. Technol., 16(2022) 1846-1855. https://doi.org/10.1016/j.jmrt.2021.12.113

[16] H. Kirchner, W. Kromp, F. Prinz, P. Trimmel, Plastic deformation under simultaneous cyclic and unidirectional loading at low and ultrasonic frequencies[J]. Mater. Sci. Eng., 68 (1985) 197-206. https://doi.org/10.1016/0025-5416(85)90409-4